ELSEVIER

Journal of Chromatography A, 943 (2002) 275–285

JOURNAL OF CHROMATOGRAPHY A

www.elsevier.com/locate/chroma

Evaluation of different nucleic acid stains for sensitive double-stranded DNA analysis with capillary electrophoretic separation

Xiaomei Yan[a], Wei Hang[b], Vahid Majidi[b], Babetta L. Marrone[a], Thomas M. Yoshida[b,*]

[a]*Bioscience Division, Los Alamos National Laboratory, Los Alamos, NM 87545, USA*
[b]*Chemistry Division, Los Alamos National Laboratory, Los Alamos, NM 87545, USA*

Received 1 June 2001; received in revised form 30 October 2001; accepted 30 October 2001

Abstract

This paper outlines the first use of SYTOX Orange, SYTO 82 and SYTO 25 nucleic acid stains for on-column staining of double-stranded DNA (dsDNA) fragments separated by capillary electrophoresis (CE). Low-viscosity, replaceable poly-(vinylpyrrolidone) (PVP) polymer solution was used as the sieving matrix on an uncoated fused-silica capillary. The effects of PVP concentration, electric field strength, and incorporated nucleic acid stain concentrations on separation efficiency were examined for a wide range of DNA fragment sizes. Our study was focused on using nucleic acid stains efficiently excitable at a wavelength of 532 nm. Among the five tested nucleic acid stains, SYTOX Orange stain was shown to have the best sensitivity for dsDNA detection by CE. About a 500-fold lower detection limit was obtained compared to commonly used ethidium bromide and propidium iodide. SYTOX Orange stain also provided a wide linear dynamic range for direct DNA quantitation with on-line CE detection. Use of SYTOX Orange stain can greatly improve the measurement of DNA fragments by CE, which will enable an expanded set of applications in genomics and diagnostics.

Keywords: Detection, electrophoresis; DNA; Dyes; Poly(vinylpyrrolidone); SYTOX Orange; SYTO 82; SYTO 25; Ethidium bromide; Propidium iodide

1. Introduction

The rapid separation time and high resolving power of capillary electrophoresis (CE) have made it a powerful method for the analyses of DNA restriction endonuclease digests and polymerase chain reaction products [1–3]. Fluorescence, rather than UV absorption, is the proven method of choice for detecting modest concentrations of double-stranded DNA (dsDNA). Typically, a monomeric intercalating dye is added to the sieving matrix and running buffers; consequently, dsDNA does not need to be prestained prior to the electrophoretic separation [4].

The practical application of CE, however, depends on the development of enhanced detection sensitivity [5,6]. An increase in sensitivity is usually obtained through improvement in the detector (avalanche photodiode versus photon multiplier tube) or the excitation source (laser versus lamp) [7]. However, it is also possible to obtain enhanced detection limits by employing fluorophores with improved spectroscopic and DNA binding properties [8–10]. Newer intercalating dyes with enhanced fluorescent prop-

*Corresponding author. Fax: +1-505-667-1321.
E-mail address: tmy@lanl.gov (T.M. Yoshida).

0021-9673/02/$ – see front matter
PII: S0021-9673(01)01452-2

erties, such as higher extinction coefficient, higher quantum yield, lower intrinsic background, and higher nucleic acid binding affinities, are currently available. From the instrumental aspect, the use of diode lasers (532 nm Nd:YAG laser, 635 or 670 nm red diode lasers) promises to bring a new level of economy and miniaturization to laser-induced fluorescence (LIF) detection for CE.

In this paper, we examine and compare the sensitivities of five nucleic acid stains (intercalating dyes) excitable at 532 nm for on-column staining using capillary electrophoresis, and report measurements of DNA–dye binding constants for defining optimal dye concentrations for CE. Ethidium bromide (EtBr) [11,12] and propidium iodide (PI) [11,13] are two common DNA stains, with an excitation maximum close to 532 nm. SYTOX Orange stain, SYTO 82, and SYTO 25 stains (trade marks of Molecular Probes) have demonstrated large fluorescence enhancement upon binding with dsDNA [14]. Single DNA fragment sizing is routinely being carried out with SYTOX Orange stain on ultrasensitive flow cytometers [14].

For DNA separation using CE, entangled polymer solutions rather than cross-linked gels are now widely used as sieving matrix [15–17]. The excellent self-coating and electroosmotic flow (EOF) suppression properties of poly(vinylpyrrolidone) (PVP) have facilitated its use as a sieving medium in an uncoated capillary for DNA separation [18,19]. The very low viscosity of PVP solutions makes replacement of the sieving matrix much easier, which is a particular advantage in multiplexed capillary electrophoresis [20]. Recently, a PVP matrix-filled microchannel has been used for separation of SYTOX Orange stain prelabeled dsDNA fragments [21]. PVP solutions have been applied in genotyping [18–20,22] and sequencing [18,23] with good resolution where the DNA fragment length was below 1000 base pairs (bp). However, the separation efficiency of PVP has been reported to be inadequate for separation of RNAs derived from individual mammalian cells, where 18S (about 2000 nucleotides) and 28S (about 5000 nucleotides) ribosomal RNAs are the most dominant components [24]. In this work, PVP was adopted as the separation matrix, to eliminate capillary treatment, and its resolving power for both short and long fragment sizes was examined. To our knowledge, this is the first demonstration of the use of SYTOX Orange, SYTO 82, and SYTO 25 stains for fluorescence detection of dsDNA separated by CE via on-column staining. The utility of SYTOX Orange stain for quantitative fragment sizing was also evaluated.

2. Experimental

2.1. Chemicals and reagents

Tris–borate–EDTA (1× TBE, 89 m*M* Tris, 89 m*M* boric acid, 2 m*M* EDTA, pH 8.3) buffer was purchased from Sigma (St. Louis, MO, USA). PVP, molecular mass 1 000 000, was obtained from Polysciences (Warrington, PA, USA). The 1 kb Plus DNA ladder (1 μg/μL) containing 20 dsDNA fragments (100–12 000 bp) was purchased from Gibco/BRL (Gaithersburg, MD, USA). Bacteriophage lambda DNA and *Hae*III digested ϕX174 DNA (1 μg/μL) were from Promega (Madison, WI, USA). The 20 bp ladder (200 ng/μL) was from BioWhittaker Molecular Applications (Rockland, ME, USA). SYTOX Orange, SYTO 82, and SYTO 25 nucleic acid stains along with propidium iodide, ethidium bromide, were purchased from Molecular Probes (Eugene, OR, USA). Deionized water was obtained from a Milli-Q system (Bedford, MA, USA).

2.2. Polymer solution and buffer preparation

A 1× TBE solution was used as the background electrolyte. PVP powder was dissolved in 1×TBE solution to yield 1.0–4.0% (w/v) polymer solutions. After addition of the powder, the mixture was vortexed for 5 min and left standing for 2 h to remove bubbles. Centrifugation was also used for fast degassing. No filtering was required before use. The polymer solutions can last more than 10 days without degradation in performance. Monomeric intercalating dyes were added to both the PVP polymer solution and the 1× TBE buffer daily. These two solutions served as the sieving matrix and running buffer, respectively.

2.3. CE fluorescence detection system

The CE fluorescence detection system consisted of a Crystal CE 310 unit (BioMolecular Instruments, Franklin, MA, USA) for sample injection and electrophoresis and a Spectrovision FD-100 fluorescence detector (Groton Technologies, Concord, MA, USA). Excitation light from a pulsed Xenon lamp passed through a 535DF35 band-pass filter (Omega Optical, Brattleboro, VT, USA) and was focused on the capillary detection window. The emitted fluorescence collected at 90° passed through a long-pass filter (565ALP, Omega Optical) and was detected by a R268 photomultiplier tube (PMT). A sliding filter assembly allowed for easy exchange of the excitation and emission filters. A Lab-PC+ Multifunction I/O board (National Instruments, Austin, TX, USA) was used to digitize the data and the electropherograms were displayed using software written in LabVIEW. Separations were performed in a 60 cm (40 cm effective length) 75 μm I.D.×375 μm O.D. bare fused-silica capillary (Polymicro Technologies, Phoenix, AZ, USA). Negative voltage (−7.5 to −20 kV) was applied at the inlet end to drive the electrophoresis; the outlet end was held at ground potential. Origin 5.0 (Microcal Software, Northampton, MA, USA) was used for data processing and simulation.

2.4. CE experimental procedure

A new capillary was flushed with 0.2 *M* HCl for 5 min and then rinsed with deionized water for 5 min. The sieving matrix was forced into the capillary under 2000 mbar pressure. Three minutes or more was required to fill the capillary, depending on the PVP concentration. During electrophoresis, both the cathodic and anodic reservoirs were filled with the running buffer solution. Between each run the column was reconditioned by flushing 0.2 *M* HCl for 2 min followed by 2 min deionized water at 2000 mbar. The capillary was refilled with the PVP-containing sieving matrix after each run. The column was stored overnight in water and rinsed each morning with 0.2 *M* HCl and deionized water for 5 min each. By preparing samples in a highly diluted buffer (low-conductivity solution), field amplified sample injection was achieved [25]. Meanwhile, sample stacking can yield on-column concentration with enhanced detectability and resolution [26]. Therefore, the DNA samples were diluted to appropriate concentrations with 0.01× TBE solution immediately before use.

2.5. Fluorometry measurement

Fluorometric titrations for DNA–dye binding constants measurements were performed using a SPEX Fluorolog-2 spectrofluorometer (JY Horbiba, Edison, NJ, USA) with a disposable 7 mm I.D. round glass cuvette (Sienco, Wheat Ridge, CO, USA).

3. Results and discussion

3.1. Evaluation of PVP separation performance

3.1.1. Effect of PVP concentration

A 1 kb Plus DNA ladder, containing 20 DNA fragments with sizes ranging from 100 to 12 000 bp, was used to evaluate the separation performance of PVP polymer. The measured entanglement threshold of PVP, molecular mass M_w=1 000 000, is reported to be 0.85% (w/w) [27]. Fig. 1 shows the electropherograms obtained with 1.0–4.0% PVP solutions with 1.0 μ*M* SYTOX Orange stain placed in both sieving and running buffers. The highest electrophoretic mobility was produced in 1.0% PVP; the relatively low viscosity of this medium produced relatively little retardation of the dsDNA. The resolving power increased initially with the increase of PVP concentration, reaching a maximum at about 3.0%. Further increases in the PVP concentration extended the retention time without additional improvement in separation efficiency. Peaks differing in size by 1 kilobase pair (kbp) were resolved for fragments as large as 9 kbp at >2.0% PVP concentrations. However, this separation was not as efficient as reported by Hammond et al. [28] for large DNA fragments, where diluted hydroxyethylcellulose (HEC, M_w=90 000–105 000) solution was used as the sieving matrix in a polyacrylamide-coated capillary. The gradually elevated baseline in 4.0% PVP was probably a result of Joule heating, which is more prominent at relatively long separation times.

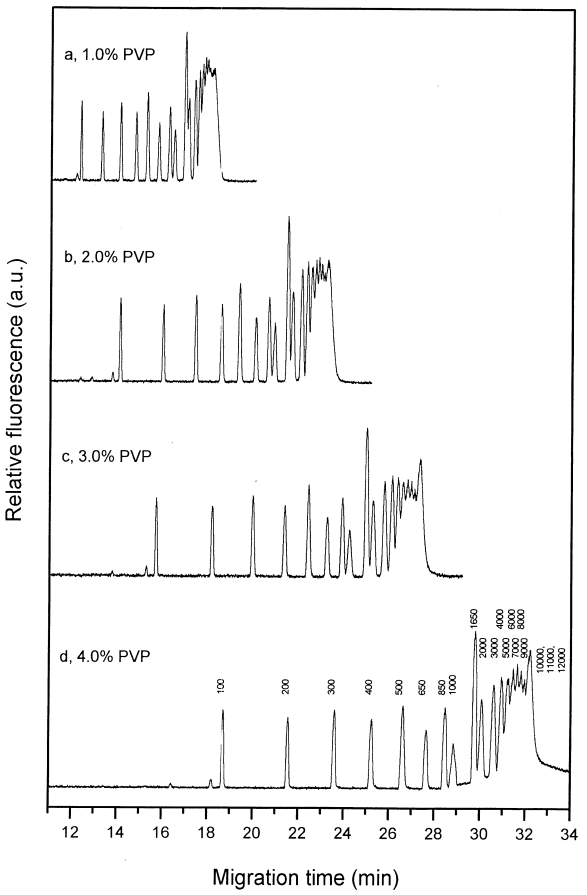

Fig. 1. Influence of PVP concentration on the separation efficiency of a 1 kb Plus DNA ladder. PVP concentration: (a) 1.0%; (b) 2.0%; (c) 3.0%; (d) 4.0%. Conditions: 1.0 μ*M* SYTOX Orange stain in both the sieving and running buffer; electric field strength, 250 V/cm; sample concentration, 2.0 ng/μL; sample injection, 167 V/cm for 6 s. a.u = Arbitrary units.

Electrophoretic mobility and the ''resolution length'' (*RSL*) calculated from data in panels (a) and (c) of Fig. 1 are plotted as a function of DNA size in Fig. 2a and b, respectively. The resolution length is the smallest difference in DNA size (base pairs) that can be resolved, which can be expressed by the following equation [29]:

$$RSL = \frac{W_h}{dx/dM} \approx \frac{W_h}{\Delta x/\Delta M} \quad (1)$$

where W_h is the peak width measured at half-maximum, and dx/dM is the first derivative of the function $x(M)$, relating the migration time x and the fragment size M. When the separation includes an array of length standards, $dx/dM \approx \Delta x/\Delta M$, where Δx is the migration time difference between two adjacent peaks, and ΔM is the size increment between these two standards. Note that the smaller the value of *RSL*, the better the performance of the separation method. Multiple Gaussian fitting was carried out to determine W_h and dx/dM for peaks up to 5 kbp. The *RSL* for larger fragments are not plotted due to the difficulty in fitting peaks >5 kbp.

Three percent PVP yielded a mobility curve with steeper slopes than 1.0% PVP (Fig. 2a), which suggested enhanced separation abilities at higher PVP concentration. In fact, better resolution (lower *RSL*) across the entire size range of the 1 kb Plus DNA ladder is shown in Fig. 2b for 3.0% PVP. A *RSL* of 3, 4, 6, 8.5, and 14 bp was obtained for the 100, 200, 300, 400, and 500 bp DNA fragments, respectively, using 3.0% PVP. However, resolution deteriorated dramatically when the fragment was greater than 500 bp. For the fragments less than 1000 bp in length, the superiority of 3.0% PVP over 1.0% PVP, in resolution power, gradually diminished with increasing fragment size. Interestingly, the *RSL* curves obtained with these two concentrations diverge with fragment size above 1000 bp. Correspondingly, two distinct slopes are apparent for each mobility curve (Fig. 2a), one for the fragments less than 1000 bp in length and one for fragments greater than 1000 bp in length. These trends indicate that two distinct sieving regimes were involved over the size range of DNA fragments tested [30]. By choosing higher polymer concentration, the resolution for both small fragments (<500 bp) and large fragments (>3 kbp) was significantly improved, but the time for separation became longer. Therefore, a PVP concentration of 3.0% was used for the following experiments.

3.1.2. Effect of applied electric field strength

Theoretically, an increase in electric field should lead to a decrease in diffusion (resulting zone broadening) due to shorter separation time. The variance contributed by diffusion is described as the following:

$$\sigma^2_{dif} = 2Dt = 2DL/v = 2DL/\mu E \quad (2)$$

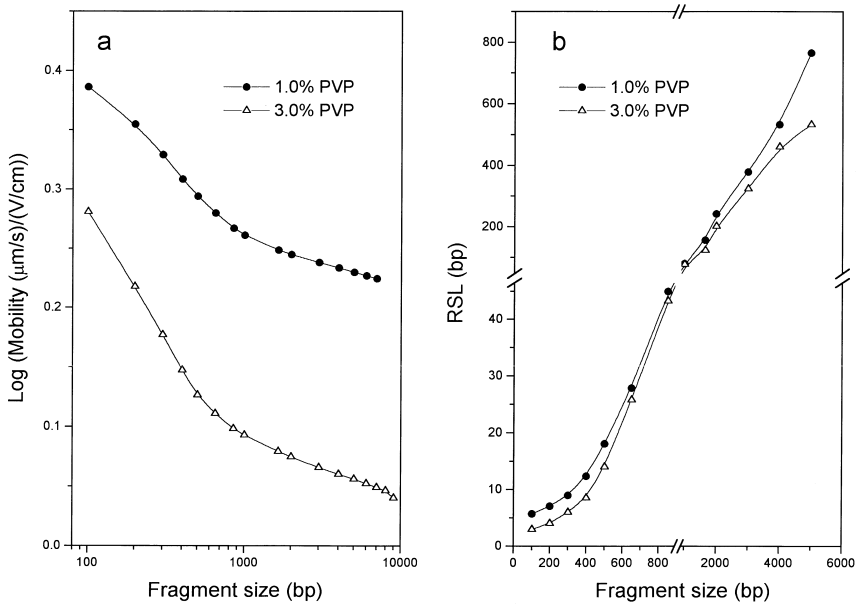

Fig. 2. Plots of DNA fragment electrophoretic mobility (a) and resolution length (i.e., the smallest difference in DNA size in bp that can be resolved) (b) as a function of fragment size for a 1 kb Plus DNA ladder separated in PVP at 1.0 and 3.0% concentrations. Data extracted from Fig. 1a and c.

with D being the molecular diffusion coefficient, t the elution time, L the length to the detector, v the velocity of the analyte, E the electric field strength, and μ the electrophoretic mobility. The separation efficiency expressed in terms of the number of ''theoretical plates'' is defined as [31]:

$$N = \frac{L^2}{\sigma_{\text{dif}}^2} = \frac{L\mu E}{2D} \tag{3}$$

which is proportional to the electric field strength E if molecular diffusion is solely responsible for zone broadening. Therefore, an increase in applied voltage will increase resolution until Joule heating becomes a problem. CE separations of the 1 kb Plus DNA ladder were carried out at four different electric fields, 125, 167, 250, and 333 V/cm, respectively (data not shown to conserve space). Significant band broadening was observed at 125 V/cm as a result of diffusion. In general, a higher voltage resulted in a shorter analysis time (21.5 min at 333 V/cm vs. 68 min at 125 V/cm) and improved separation efficiency. The onset of appearance of resolved peaks for fragments of 4, 8, and 9 kbp was observed at 125, 167, and 250 V/cm, respectively. Peaks above 10 kbp with 1 kbp size differences were not resolved at any field strength. The best resolution was obtained at 250 V/cm, which was chosen as the field strength for the next series of experiments.

3.1.3. Resolving power for short fragments

The separation performance of PVP solution for shorter dsDNA fragments was examined using a 20 bp ladder with the electropherogram shown in Fig. 3. This ladder consisted of 50 fragments covering the range of 20 to 1000 bp in 20 bp increments. The 200 and 500 bp fragments were present at an increased amount relative to the other fragments to serve as internal reference indicators. Below 500 bp, fragments differing in size by 20 bp were clearly resolved, which agreed very well with the resolution plot shown in Fig. 2b. This 20 bp ladder was a DNA marker prepared for gel electrophoresis, so it was not a surprise that smaller peaks appeared in between prominent peaks upon CE separation. The unidentified peaks were more obvious below 300 bp corresponding to the great resolution exhibited by the current PVP sieving protocol. However, above 500

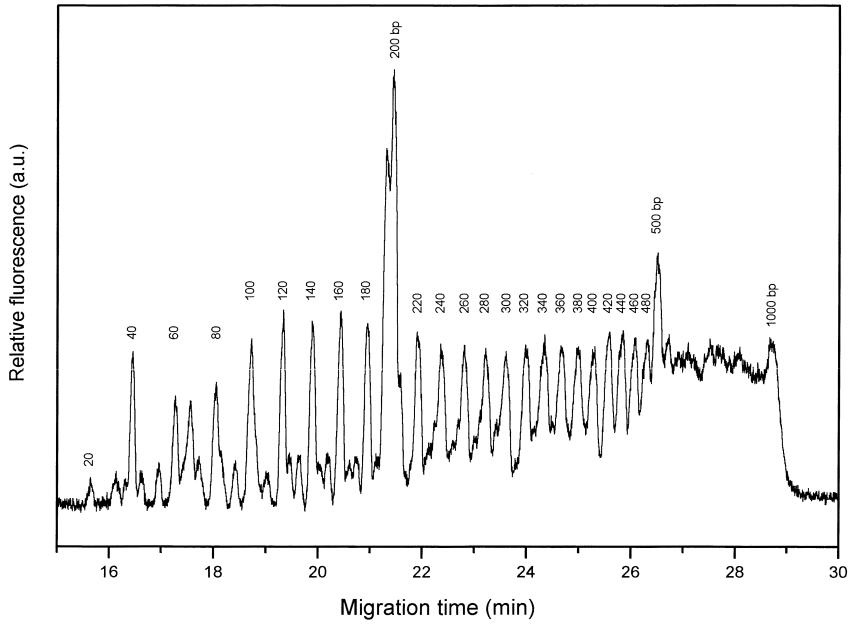

Fig. 3. Capillary electrophoresis separation of a 20 bp ladder. Conditions: PVP concentration, 3.0%; SYTOX Orange concentration, 1.0 μ*M*; electric field strength, 250 V/cm; sample concentration, 2.0 ng/μL; sample injection, 83 V/cm for 12 s.

bp our resolving power was not as good as that reported by Gao and Yeung [18], where 27 alleles of a D1S80 ladder ranging from 369 to 801 bp with 16 bp between adjacent alleles were baseline resolved.

3.2. SYTOX Orange stain for CE-separated dsDNA detection

3.2.1. Concentration effect

In the previous experiments a SYTOX Orange stain concentration of 1.0 μ*M* was used for on-column staining. In this section, the effect of SYTOX Orange concentration on the sensitivity and efficiency of CE-separated dsDNA fragments was investigated using a *Hae*III digest of ϕX174 DNA, which contains 11 different restriction fragments ranging in size from 72 to 1353 bp. Fig. 4 shows the electropherograms obtained with six different SYTOX Orange concentrations (0.2, 0.5, 1.0, 2.0, 5.0, and 10.0 μ*M*) at a DNA concentration of 1.0 ng/μL and a PVP concentration of 3.0%. Clear separations were obtained for most of the dye concentrations (except 0.2 μ*M*) within a reasonable time scale, and 271 and 281 bp fragments were completely resolved when the SYTOX Orange concentration was above 1.0 μ*M*. At a SYTOX Orange concentration of 0.2 μ*M*, the 1078 and 1353 bp fragments were not resolved, resulting in a broad peak. In general, we found that the electrophoretic mobility decreased with an increase in dye concentration. This could be attributed to changes in the combined mass and charge due to dye–DNA complex formation. Slightly better resolving power was obtained with longer retention times at higher dye concentrations.

The fluorescence intensity of the DNA fragments initially increased with increasing dye concentration up to 1.0 μ*M* and then declined at higher SYTOX Orange concentrations. The injected ϕX174/*Hae*III sample concentration was 1.0 ng/μL, which corresponds to a DNA fragment concentration of 0.25 ng/μL for the largest DNA fragment (the longest digested fragment, 1353 bp, is 25% of the total 5386 bp length of ϕX174 DNA). During the electrophoretic separation, band broadening (due to diffusion, Joule heating, adsorption and other possible sources) and narrowing (due to sample stacking) occurred for each size of fragments. The resultant Gaussian peak shape reflected a concentration distribution for each band, therefore the true concen-

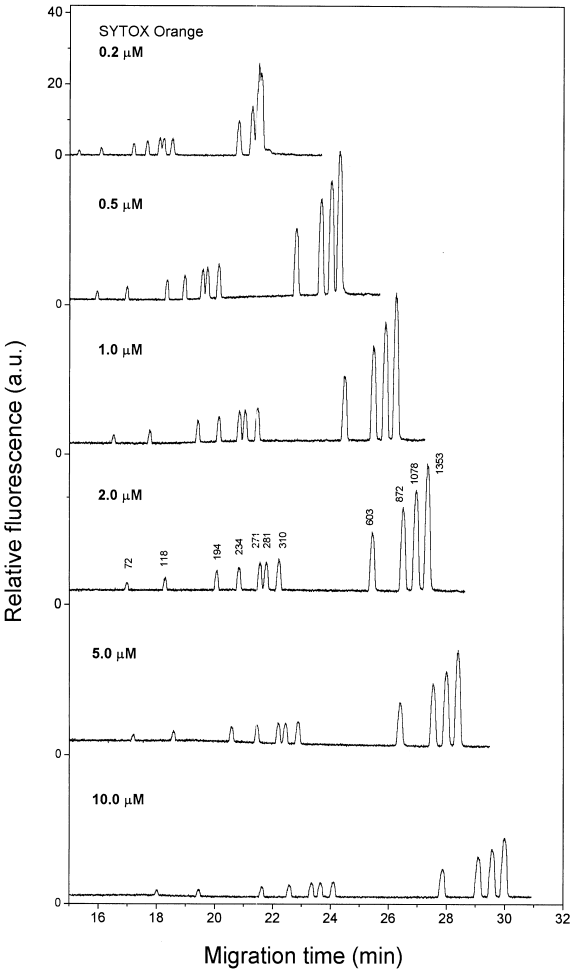

Fig. 4. Capillary electrophoresis separation of a *Hae*III digested ϕX174 DNA as a function of SYTOX Orange concentration placed in both the sieving and running buffer. Sample concentration, 1.0 ng/μL; sample injection, 83 V/cm for 6s. Other conditions as in Fig. 3.

tration of the DNA at the detection window was not known. Nevertheless, if we assume that the band concentration did not change upon electrophoresis, a 0.25 ng/μL concentration of DNA only contained 0.19 μ*M* of intercalative binding sites (0.25 ng/μL = 0.38 μ*M* bp, and one intercalative site of a mono-intercalating dye covers 2 bp). Even though 100% intercalation efficiency was achieved via on-column staining, the free dye concentration was about the same as the incorporated dye concentration for dye concentrations above 2.0 μ*M*.

Significant differences in the behavior of dye molecules in aqueous solution and polymer solution were observed. A model describing two binding modes, intercalation (primary, yielding fluorescence) and external binding (secondary, involving fluorescence quenching), has been proposed to interpret DNA and intercalating dye interactions in aqueous solution [14]. The equilibrium dissociation constant K_{D2} for secondary binding was measured as 2.1 μ*M* for SYTOX Orange stain in 1× TE buffer (10 m*M* Tris–HCl, 1 m*M* EDTA). Therefore, if the free dye concentration was equal to K_{D2}, the signal should have been quenched by 50%. Although fluorescence quenching was observed in PVP at SYTOX Orange concentrations above 2.0 μ*M*, the extent was not as significant as that observed in aqueous solution. This can probably be attributed to the shielding effect of the PVP entangled polymer network. At a higher viscosity (~12.5 cP at 3.0% PVP, Ref. [18]), the free dye molecules cannot gain access to the DNA fragments as freely as in aqueous solution due to diffusion limitation. Therefore, the dissociation constant for the DNA–dye interaction was dependent on the buffer environment. In addition, the dynamic cross migration of dye molecules and DNA fragments for on-column staining further complicates the interpretation of DNA–dye binding during capillary electrophoresis.

3.2.2. Quantitation capability

Quantitation of DNA by capillary electrophoresis has been described by several research groups [32–34]. Using ϕX174/*Hin*cII digest as an internal standard, Nathakarnkitkool et al. [32] analyzed a 361-bp segment of an androgen receptor mRNA transcript in less than 20 min with a peak area RSD of 3.06% ($n = 6$). We evaluated the capability to quantitate DNA with SYTOX Orange stain by analyzing serial dilutions of ϕX174/*Hae*III digest. The 11 DNA fragments in the ϕX174/*Hae*III digest represent a nearly 20-fold (1353 bp/72 bp) range of DNA concentrations.

Fig. 5 shows the electropherograms with the plots of integrated peak area as a function of known fragment size. Note that the *y*-axis is scaled proportionally to the injected ϕX174/*Hae*III sample concentration. Because DNA bands move through the sieving buffer at different rates, the area was

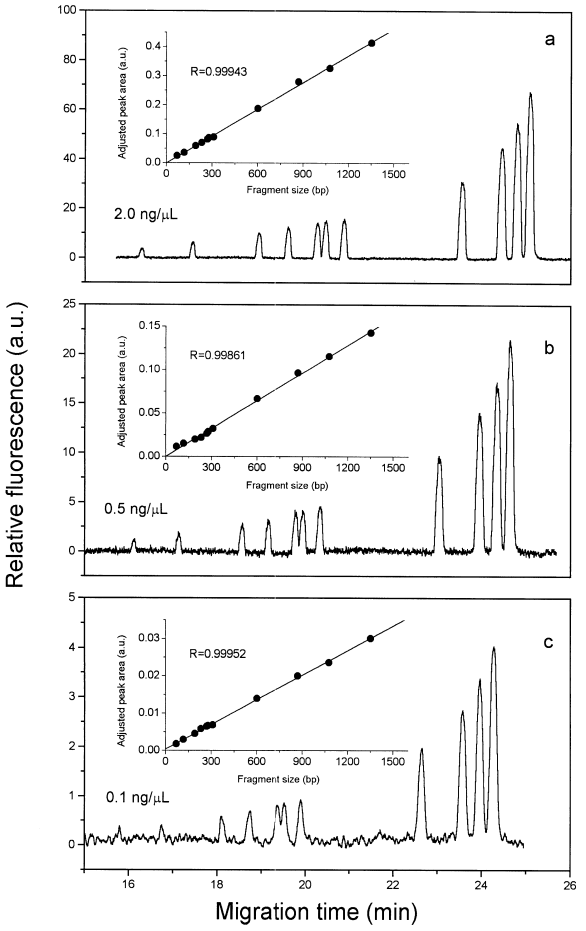

Fig. 5. Capillary electrophoresis separations of three different concentrations of *Hae*III digested ϕX174 DNA. The electropherogram shown in (c) was smoothed by seven adjacent averaging. Baselines have been subtracted to zero for each electropherogram. The inserts in each panel depict the linear regression plot of the normalized peak area vs. size (in bp) of each fragment. Sample injection, 83 V/cm for 6 s. Other conditions as in Fig. 3.

divided by the migration time to normalize each peak. This adjusted area, rather than peak height, has been recommended for free zone CE quantitation [35]. The highest DNA fragment concentration in the sample reservoir was 0.5 ng/μL for the 1353 bp fragments in Fig. 5a, and the lowest DNA concentration for a discernable fragment peak was 1.3 pg/μL, the 72 bp peak shown in Fig. 5c. A linear relationship was observed between the number of bound SYTOX Orange (measured by the normalized peak area) and the size (in bp) of the dsDNA fragment for each injected sample concentration, indicating uniform dye binding to dsDNA. For a restriction enzyme digest the DNA concentration of each group of fragments is proportional to the fragment size, therefore a linear response of peak area versus DNA concentration (quantitation curve) was established. The overlapped DNA fragment concentration among the three linear quantitation curves indicates that about a 400-fold linear dynamic range was obtained in the present detection system by employing 1.0 μ*M* of SYTOX Orange stain. Due to potential saturation of the fluorescence detector, concentrations of ϕX174/*Hae*III higher than 2.0 ng/μL were not tested. The addition of DNA size standards of known concentration allowed both the accurate measurement of fragment length as well as the quantitative determination of analyte DNA segments. However, co-injection of analyte and standard may be required to avoid the bias associated with electrokinetic injection due to field amplified sample injection and sample stacking.

If the equilibrium dissociation constant, K_{D1}, for SYTOX Orange and DNA intercalation is known, the quantitation curves for different dye concentrations can be simulated. The concentration of DNA–dye complex $[LR_1]$ via primary binding can be solved through the following quadratic equation [14]:

$$[LR_1]^2 - ([R_1]_{tot} + [L]_{tot} + K_{D1}) \times [LR_1] + [R_1]_{tot} \times [L]_{tot} = 0 \quad (4)$$

where L is the ligand (dye molecule) for intercalation, which covers 2 bp for a monomeric intercalating dye; R_1 is the receptor for primary binding (intercalative DNA-binding site); and $[L]_{tot}$ and $[R_1]_{tot}$ are the total concentrations of dye molecules and intercalative binding sites, respectively. A K_{D1} of 1.69 n*M* was measured in TE buffer [14]. As discussed above, the polymer solution with elevated viscosity changes the DNA–dye binding constant; therefore, simulations with a 20-fold higher K_{D1} were also carried out.

Fig. 6 shows the simulated DNA quantitation

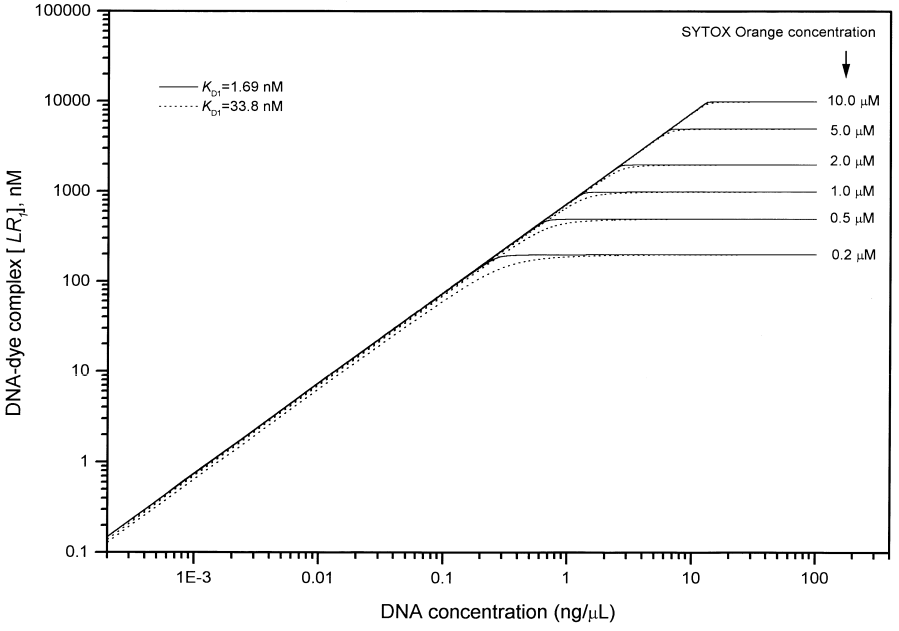

Fig. 6. Simulated DNA quantitation curves for six different SYTOX Orange concentrations. The equilibrium dissociation constants K_{D1} of 1.69 n*M* (———) and 33.8 n*M* (· · ·) were used.

curves for six different SYTOX Orange concentrations. The potential fluorescence quenching at high free dye concentrations was not taken into account during simulation. The solid and dotted lines were obtained for K_{D1} of 1.69 and 20·1.69 n*M* (33.8 n*M*), respectively. Since the fluorescence signal observed during the quantitation experiment was directly proportional to the concentration of the DNA–dye complex, here the *y*-axis of the quantitation curve is given as DNA–dye complex concentration. As shown in Fig. 6, when the DNA concentration is relatively low, the amount of DNA–dye complex increases linearly with the increase of DNA concentration, which yields a linear quantitation curve. With a further increase in DNA concentration, all the dye molecules are gradually consumed via intercalation and eventually the concentration of DNA–dye complex stabilizes regardless of the continuing increased DNA concentrations. For the 1.0 μ*M* SYTOX Orange concentration used above, the linear quantitation curve for DNA fragments in the sample reservoir should be able to extend up to a concentration of 1.0 ng/μL if not limited by detector saturation.

3.3. SYTOX Orange sensitivity comparison with other nucleic acid staining dyes

A comparison of detection sensitivity among five nucleic acid stains for on-column staining of CE-separated DNA fragments is shown in Fig. 7. To circumvent the limited detector dynamic range, *Hae*III digested ϕX174 DNA stock was diluted appropriately for each nucleic acid stain while maintaining the same injection condition. As indicated by the simulated quantitation curves (Fig. 6), proper selection of dye concentration for staining is essential for unbiased sensitivity comparisons. Each band concentration of CE-separated DNA fragments should fall into the linear dynamic range of the quantitation curve to avoid under-staining. In other words, intercalation efficiency close to 100% is desired for each fragment. Although higher dye concentrations are preferable for quantifying higher

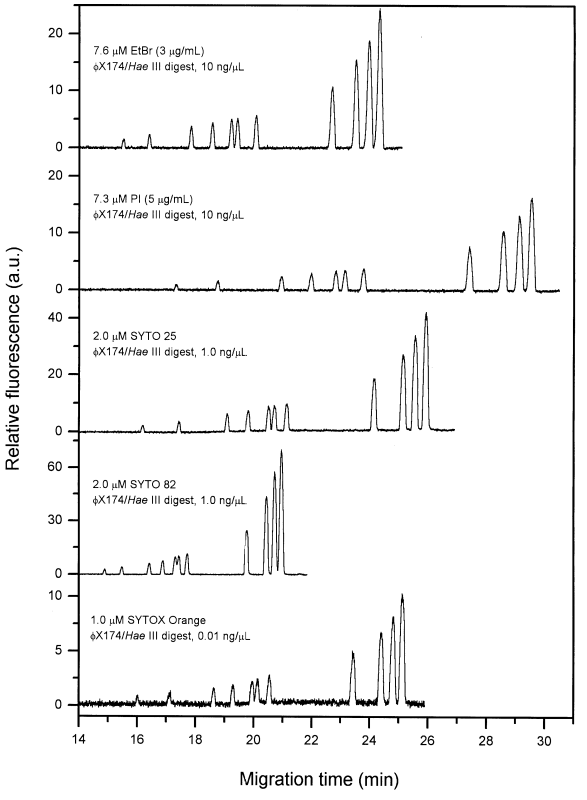

Fig. 7. Capillary electrophoresis separations of *Hae*III digested ϕX174 DNA with five different nucleic acid stains. See panel legend for dye and DNA concentration information. Sample injection, 167 V/cm for 18 s. Other conditions as in Fig. 3.

DNA concentrations, a compromise exists since fluorescence quenching also increases at higher dye concentration. The equilibrium dissociation constants for both primary and secondary DNA–dye binding modes were measured with a spectrofluorometer as described in our earlier report [14]. Table 1 summarizes the maximum excitation and emission wavelength, primary and secondary equilibrium dissociation constants for two modes of DNA–intercalating dye interactions, and the calculated detection limits for each nucleic acid stain based on $3\times\sigma$ (background noise) and peak heights of data shown in Fig. 7. The intercalation-binding constant for ethidium bromide was found to be 100 n*M*, which was about 10-fold lower than the previous report [36]. Propidium iodide has an additional quaternary ammonium ion and a charge of +2. Consequently, propidium iodide had ~10-fold higher DNA affinity than

Table 1
Fluorescence property comparison among five 532 nm wavelength excitable nucleic acid stains

Nucleic acid stain	$\lambda_{Ex}/\lambda_{Em}$ [a] (nm)	K_{D1} [b] (n*M*)	K_{D2} [b] (n*M*)	Detection [c] limits (pg/μL)
EtBr	518/605	100	>70 000	29.2
PI	535/617	10	>70 000	37.4
SYTO 25	521/556	20	4000	2.6
SYTO 82	541/560	40	4000	1.4
SYTOX Orange	547/570	1.69	2150	0.072

[a] Excitation and emission maxima determined in the presence of DNA. Data obtained from Molecular Probes, www.probes.com.

[b] K_{D1} and K_{D2} denote primary and secondary dissociation constants, respectively. Measurements were made in 10 m*M* HCl, 1 m*M* EDTA buffer with bacteriophage lambda DNA. For detailed experimental information, see Ref. [14].

[c] See text for experimental details.

ethidium bromide (K_{D1} about 10 n*M*). The larger than 70 μ*M* K_{D2} for ethidium bromide and propidium iodide indicates that the occurrence of fluorescence quenching will not be encountered under normal staining conditions. The incorporated dye concentration for each nucleic acid stain in Fig. 7 was chosen based on the prerequisites discussed above.

Excellent separations were obtained for all five nucleic acid stains with associated different electrophoretic mobility. All DNA fragments migrated more rapidly in the presence of ethidium bromide than in the presence of propidium iodide, which was in agreement with the previous report by Kim and Morris [11]. Excellent correlations between peak height and fragment length indicated that the fragment concentrations fell along the linear quantitation curve offered by each dye concentration. Despite having the lowest K_{D2}, SYTOX Orange exhibited the highest detection sensitivity for DNA on-column staining, presumably due to its large fluorescence enhancement upon binding to dsDNA. Compared to the more commonly used EtBr or PI, SYTOX Orange stain was about 500-fold more sensitive for DNA detection in our study. SYTO 82 provided the second highest sensitivity, followed by SYTO 25. EtBr and PI shared similar sensitivities for on-column DNA staining. With SYTOX Orange stain and lamp excitation, the detection limit of DNA concentration in the sample solution was 0.072 pg/μL. If laser-induced fluorescence is implemented, the

application of SYTOX Orange dye as an on-column stain for CE-separated dsDNA fragments is very promising for ultrahigh sensitivity detection.

4. Conclusions

In summary, PVP solution provided an acceptable electrophoretic separation for a wide size range of dsDNA fragments on an uncoated capillary. SYTOX Orange stain was applied for the first time as an on-column staining reagent for DNA fragments separated by capillary electrophoresis. Greatly enhanced (~500-fold) sensitivity has been demonstrated compared to EtBr or PI. Based on our simulation, a linear detection range of over three orders of magnitude DNA concentration could be obtained with SYTOX Orange stain for direct capillary electrophoresis quantitation. SYTOX Orange dye is an excellent dye of choice for highly accurate and sensitive CE analysis of DNA fragments.

Acknowledgements

This work was supported by the Chemical and Biological Nonproliferation Program (NN-20) of the Department of Energy, and by the FBI Hazardous Materials Response Unit, for which we are most grateful. The statements and conclusions herein are those of the authors and do not necessarily represent the views of the FBI.

References

[1] A. Guttman, N. Cooke, Anal. Chem. 63 (1991) 2038.
[2] M. Strege, A. Lagu, Anal. Chem. 63 (1991) 1233.
[3] N. Zhang, E.S. Yeung, J. Chromatogr. A 768 (1997) 135.
[4] H.E. Schwartz, K.J. Ulfelder, Anal. Chem. 64 (1992) 1737.
[5] X.H.C. Huang, M.A. Quesada, R.A. Mathies, Anal. Chem. 64 (1992) 967.
[6] R.S. Madabhushi, M. Vainer, V. Dolnik, S. Enad, D.L. Barker, D.W. Harris, E.S. Mansfield, Electrophoresis 18 (1997) 104.
[7] C.V. Owens, Y.Y. Davidson, S. Kar, S.A. Soper, Anal. Chem. 69 (1997) 1256.
[8] H. Zhu, S.M. Clark, S.C. Benson, H.S. Ray, A.N. Glazer, R.A. Mathies, Anal. Chem. 66 (1994) 1941.
[9] D. Figeys, E. Arriaga, A. Renborg, N.J. Dovichi, J. Chromatogr. A 669 (1994) 205.
[10] J. Skeidsvoll, P.M. Ueland, Anal. Biochem. 231 (1995) 359.
[11] Y. Kim, M.D. Morris, Anal. Chem. 66 (1994) 1168.
[12] M.A. Stebbins, C.R. Schar, C.B. Peterson, M.J. Sepaniak, J. Chromatogr. B 697 (1997) 181.
[13] T. Godard, E. Deslandes, P. Lebailly, C. Vigreux, L. Poulain, F. Sichel, J.M. Poul, P. Gauduchon, Cytometry 36 (1999) 117.
[14] X. Yan, R.C. Habbersett, J.M. Cordek, J.P. Nolan, T.M. Yoshida, J.H. Jett, B.L. Marrone, Anal. Biochem. 286 (2000) 138.
[15] A.G. Ewing, R.A. Wallingford, T.M. Olefirowicz, Anal. Chem. 61 (1989) 292A.
[16] B. Braun, H.W. Blanch, J.M. Prausnitz, Electrophoresis 18 (1997) 1994.
[17] M.P. Richards, C.M. Ashwell, J.P. McMurtry, J. Chromatogr. A 853 (1999) 321.
[18] Q. Gao, E.S. Yeung, Anal. Chem. 70 (1998) 1382.
[19] Q. Gao, H. Pang, E.S. Yeung, Electrophoresis 20 (1999) 1518.
[20] Q. Gao, E.S. Yeung, Anal. Chem. 72 (2000) 2499.
[21] Z. Ronai, C. Barta, M. Sasari-Szekely, A. Guttman, Electrophoresis 22 (2001) 294.
[22] N. Zhang, H. Tang, E.S. Yeung, Anal. Chem. 71 (1999) 1138.
[23] J. Song, E.S. Yeung, Electrophoresis 22 (2001) 748.
[24] F. Han, S.J. Lillard, Anal. Chem. 72 (2000) 4073.
[25] R.L. Chien, D.S. Burgi, J. Chromatogr. 559 (1991) 141.
[26] A. Vinther, H. Soeberg, J. Chromatogr. 559 (1991) 27.
[27] B. Braun, H.W. Blanch, J.M. Prausnitz, Electrophoresis 18 (1997) 1994.
[28] R.W. Hammond, H. Oana, J.J. Schwinefus, J. Bonadio, R.J. Levy, M.D. Morris, Anal. Chem. 69 (1997) 1192.
[29] C. Heller, Electrophoresis 20 (1999) 1978.
[30] B.A. Siles, D.E. Anderson, N.S. Buchanan, M.F. Warder, Electrophoresis 18 (1997) 1980.
[31] J.W. Jorgenson, K.D. Lukacs, Anal. Chem. 53 (1981) 1298.
[32] S. Nathakarnkitkool, P.J. Oefner, G. Bartsch, M.A. Chin, G.K. Bonn, Electrophoresis 12 (1992) 18.
[33] H.E. Schwartz, K. Ulfelder, F.J. Sunzeri, M.P. Busch, R.G. Brownlee, J. Chromatogr. 559 (1991) 267.
[34] M. Huang, S. Liu, B.K. Murray, M.L. Lee, Anal. Biochem. 207 (1992) 231.
[35] J.M. Butler, B.R. McCord, J.M. Jung, M.R. Wilson, B. Budowle, R.O. Allen, J. Chromatogr. B 658 (1994) 271.
[36] B. Gaugain, J. Barbet, N. Capelle, B. Roques, J.B. LePecq, Biochemistry 17 (1978) 5078.